



# CHANGE OF EXPERIMENTAL YOUNG'S MODULUS WITH INCREASING TEMPERATURE FOR AN ABS MATERIAL SUBJECTED TO TENSILE TEST

A. En-Naji<sup>1</sup>, N. Mouhib<sup>1,2</sup>, M. Lahlou<sup>1</sup>, H. Farid<sup>3</sup> and M. El Ghorba<sup>1</sup>

<sup>1</sup>Laboratory of Control and Mechanical Characterization of Materials and Structures, National Higher School of Electricity and Mechanics, BP Oasis, Hassan II University, Casablanca, Morocco

<sup>2</sup>ISEM/Higher Institute of Maritims Studies, Road El Jadida Casablanca, Morocco

<sup>3</sup>Laboratoire de Nanotechnologie et Bioplasturgie, Université du Québec en Abitibi-Témiscamingue UQAT, boulevard de l'Université, Rouyn-Noranda, Québec J9X 5E4, Canada

E-Mail: [abdenaji14@gmail.com](mailto:abdenaji14@gmail.com)

## ABSTRACT

This article presents the decrease of Young's modulus as a function of increasing temperature in two main zones: the industrial zone of which the temperature is below the glass temperature  $T_g = 110^\circ \text{C}$ . and the thermoforming zone from which the temperature is above the same glass temperature. In the industrial zone, an experimental model namely static damage made it possible to distinguish three stages of damage. Therefore, be able to intervene in time for predictive maintenance. This study also includes a comparison between the static damage and damage by unified theory (theoretical). The comparison shows that the experimental damage is considered to be the most critical compared to theoretical. In the thermoforming zone, we adopted the same methods to follow the process of flow as a function of the temperature increase, based on the variation of Young's modulus. Likewise, we compared theoretical and experimental values which show that, unlike the previous zone, experimental damage in this area is less dangerous than the theoretical one for high loading levels.

**Keywords:** damage, flow, mechanical behavior, polymer, temperature, tensile tests, young's modulus.

## 1. INTRODUCTION

The Polymer materials used in the industries present a precious combination of properties, such as: the Corrosion resistance, the high modulus of elasticity and rigidity as regards their density, good heat and electric insulation, excellent conception (design) of shape and formability [1].

The mechanical behavior of the polymers is characterized by a very great apparent diversity. Indeed, for the same conditions of use, and from a technological point of view, polymers could be either rigid fragile or ductile or rubbery. Thus, in the family of polymers, a large number of types of behavior can be found: viscoelastic, hyper elastic, hardening, damaging. This diversity is found, for the same polymer, if some of its characteristics are varied, or even its conditions of use. This does not mean that the behavior of a polymer is variable, even uncontrolled. It is the parameters controlling its behavior and the elementary processes that are numerous [2]. Among these polymers, there is Acrylonitrile Butadiene Styrene (ABS) that is an amorphous polymer manufactured by mass emulsion or polarization of Acrylonitrile and styrene in the presence of Polybutadiene [3]. The most important properties of ABS by which it is recognized are its good impact resistance, scratch resistance, aging ability, excellent appearance and ability to be decorated. The ABS is composed of three monomers: Acrylonitrile, butadiene and styrene [4]

It is the preferred material for rapid prototyping, molded parts for the manufacture of household appliances, toys, automotive parts and computer hardware. Rapid prototyping integrates three essential concepts: time, cost and complexity of shapes [5]. This work is dedicated firstly to study the influence of temperature on the mechanical behavior of the ABS material especially his Young's modulus, by carrying out several tensile tests at a temperature which varies from ambient ( $25^\circ \text{C}$ ) to  $170^\circ \text{C}$ , near the melting temperature ( $195^\circ \text{C}$ ). Then, to evaluate damage and flow using expressions resulting from the unified theory and based on Young's modulus change with increasing temperature, namely static and theoretical damage and flow in the industrial zone (the temperature is below the glass temperature  $T_g=110^\circ \text{C}$ ) and in the thermoforming zone (the temperature is above the glass temperature  $T_g=110^\circ \text{C}$ ).

## 2. MATERIAL AND EXPERIMENTAL METHODS

The material used in this work is Acrylonitrile Butadiene Styrene (ABS). The latter is an amorphous polymer produced by emulsification or mass polymerization of Acrylonitrile and styrene in the presence of Polybutadiene emulsion.

The geometry and dimensions of the specimen used are given in Figure-1 according to ASTM D638-03 [6].

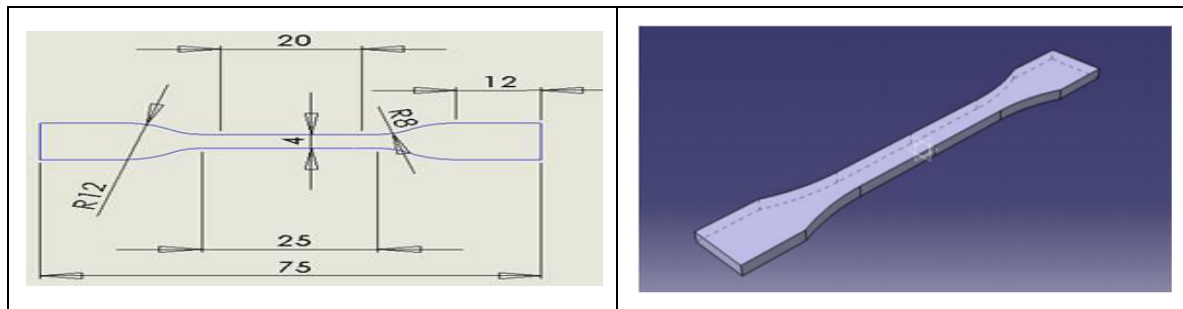


**Figure-1.** Dimensions of the specimens according to ASTM D638-03 [6].

Figure-2 shows the evolution of the stress applied to the specimens (MPa) as a function of the deformation  $\varepsilon$

(%). The general appearance of this curve has shown ductile behavior

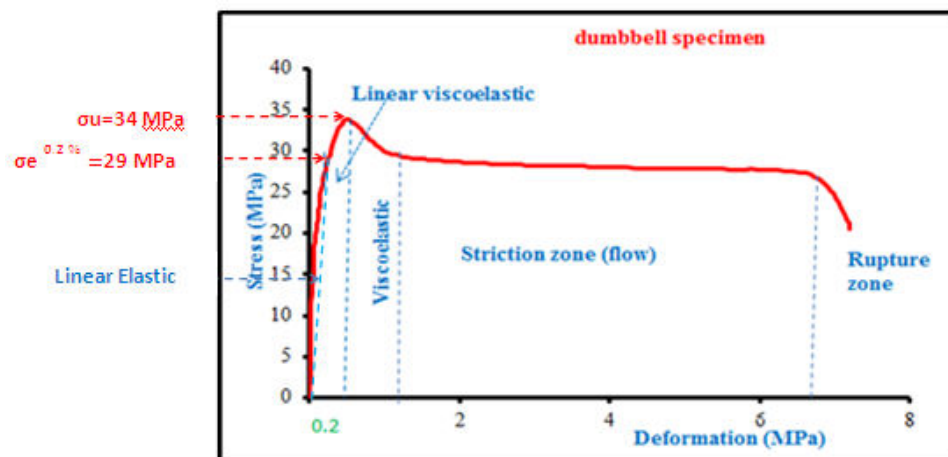


**Figure-2.** Tensile curve stress-Deformation Dumbbell specimens.

We note from Figure-2 that the curve has four zones. Each of these zones reveals a particular mechanical behavior of the material (ABS) during the tensile test.

Zone 1 (linear): this is the reversible elastic deformation of the material due to the amorphous phase.

Zone 2: the force decreases, it is the beginning of the constriction which corresponds to a heterogeneous deformation of the material

Zone 3: increase of the zone of constriction along the specimen until stabilization.

Zone 4: the stretching force increases, the deformation again becomes homogeneous thanks to a

structural hardening linked to the orientation of the macromolecular chains in the direction of stretching and the increase of the fibrillar fraction of the material until rupture.

The results shown in Figure 2 enabled us to determine the mechanical properties of the studied material.

Among these properties, we have the elastic limit, the modulus of elasticity and the breaking stress which have been given in Table-1.

**Table-1.** The mechanical characteristics of ABS.

Young's modulus	Poisson's ratio	Elastic limit	Ultimate stress
E=2 GPa	$\nu = 0,3$	$\sigma_e = 29\text{MPa}$	$\sigma_U = 34\text{ MPa}$

### 3. RESULTS AND DISCUSSIONS

#### 3.1 Temperature effect on the mechanical behavior for ABS

To take account of the influence of temperature on the mechanical characteristics of the ABS, especially

the Young's modulus, several series of tests were carried out on dumbbell specimens in a temperature range from 25°C (laboratory temperature) Up to 170°C through the glass transition temperature  $T = 110^\circ\text{C}$ .

Figure-3 Shows the evolution of Young's modulus (MPa) as a function of temperature ( $^\circ\text{C}$ ).

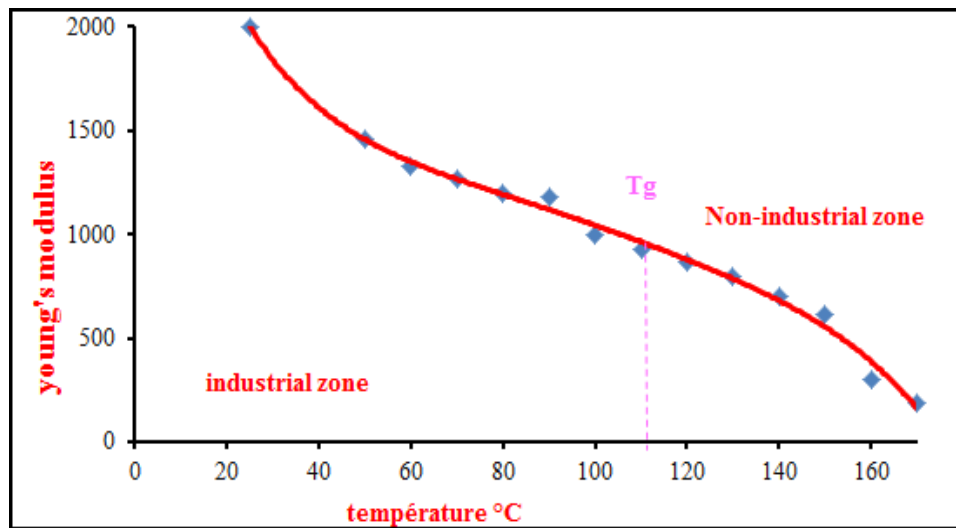


Figure-3. Loss of the Young's modulus according to the temperature [7].

On the one hand, we note the variation of the Young's modulus degradation in a remarkable way: a sudden decrease with the increase in temperature, this decrease accelerates once the glass transition temperature range is exceeded. Which is in the region of 110 ° C., on the other hand, we have seen the existence of two zones: The zone I correspond to the temperature which lies between the lab temperature  $T_a = 25^\circ \text{C}$  and the glass transition temperature  $T_g = 110^\circ \text{C}$ . Corresponding to a rigid (glassy) state, The molecules of the amorphous part are deformable (industrial zone). The zone II is above the glassy temperature and corresponds to a transition state in which movements of the chains become possible which allows greater and easier deformations. The mechanical properties drop in this phase that is to say that the mechanical behavior of the polymers is affected. This is a thermoforming zone.

### 3.2 Determination of damage in the industrial zone (25°C to 110 °C)

The static damage-reliability model consists in determining the evolution of damage as a function of fraction of life  $\beta$ :

Such as:

$$\beta = \frac{T_i - T_a}{T_g - T_a} \quad (1)$$

Where:

**T<sub>a</sub>**: ambient temperature  
**T<sub>i</sub>**: Instantaneous temperature  
**T<sub>g</sub>**: Glassy temperature

### Loss of Young's modulus

The static damage model consists in determining the variations of the Young's Modulus; these variations are essentially due to damage. Young's Modulus is usually defined [8], as being the internal forces which remain in the mechanical parts when the latter is not subjected to any external stress.

We deduct that the mechanical properties of the studied material (ABS) are influenced by temperature and consequently the material tends to become more fragile. The results are presented in the Figure-4.

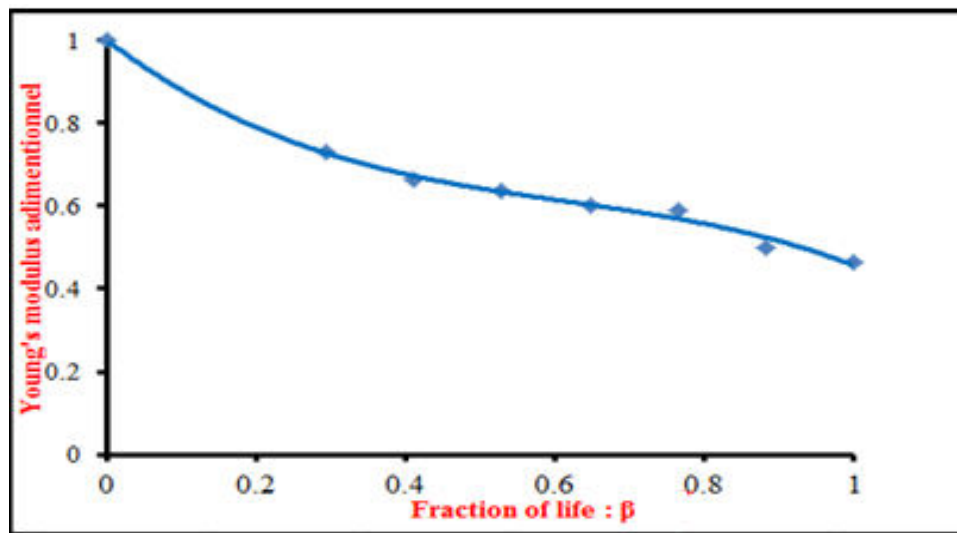


**Figure-4.** Loss of the Young's Modulus according to the fraction of life.

ABS has Young's modulus at ambient temperature of 2000MPa ( $E_{Ti} / E_{amb} = 1$ ). This dimensionless ratio decreases remarkably as a function of the life fraction  $\beta$  until it reaches a value of 0.43 for a life fraction equal to 1, which has a critical temperature, beyond which the material presents no significant resistance.

The shape of the curve in the interval  $\beta = (0 \text{ to } 0.25)$  seems to indicate that the molecular chains are deformed: the relative very low evolution of the mobility of the molecular chains, the mechanical behavior of the material behaves like a fragile material. The increase in temperature can above all increase the mobility and deformation of the molecular chains in the polymer to subsequently generate ( $\beta > 0.25$ ) a plasticizing phase which is more decisive for the amplitude of loading  $E_a$ . These general patterns of deterioration of the Young's modulus ratio in the polymer it possible to explain the faster failure rate (loss of resistance) of the stressed specimens.

#### Quantification of static damage

The static damage based on Young's Modulus, has been developed to predict the damage evolution and the artificial preloading impact which is represented by

temperature variation. The static damage model is presented in the equation (2) [9]:

$$DS = \frac{1 - \frac{E_{Ti}}{E_{amb}}}{1 - \frac{E_a}{E_{amb}}} \quad (2)$$

Where:

$E_{ambient}$ : Young's modulus at  $T = 25^\circ \text{C}$

$E_{Ti}$ : The value of the Young's Modulus for different temperatures

$E_a$ : applied Young's modulus

Static damage as a function of fraction of life is represented by the curve in figure 5, which corresponds to the deterioration of the ABS with the increase of the temperature (Figure-5) with the following conditions:

- In the initial state:  $\beta = 0 \rightarrow E_{Ti} = E_{amb} \rightarrow D = 0$
- In the final state:  $\beta = 1 \rightarrow E_{Ti} = E_a \rightarrow D = 1$

The variation of the static damage according to the life fraction is illustrated by the curve in Figure-5:

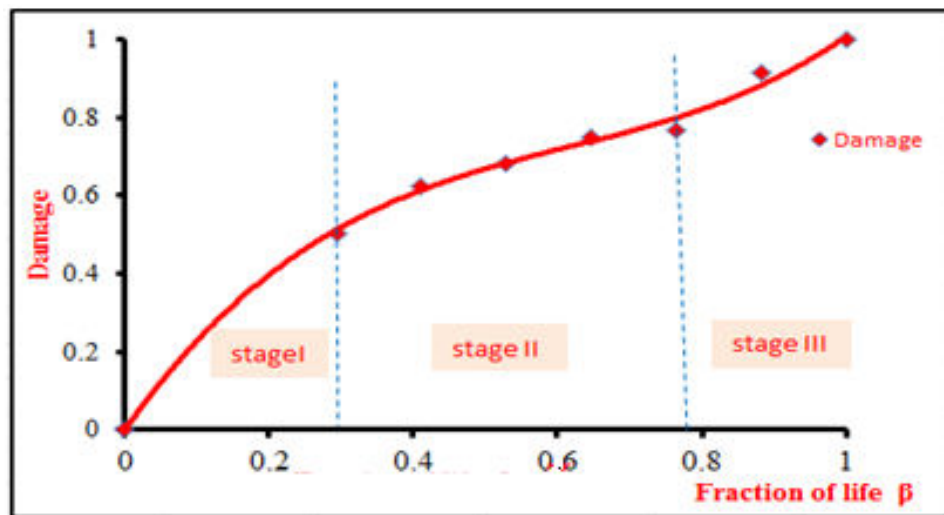


**Figure-5.** Evolution of the static damage depending on the life fraction  $\beta$ .

Figure-5 shows the evolution of the normalized experimental damage as a function of  $\beta$ . The damage gradually increases from 0 (laboratory temperature) to its critical value 1 glass temperature.

The shape and level of the damage at break gives this model experimental damage ( $D = 1$ ,  $\beta = 1$ ) some credibility, which agrees with the literature in an equivalent study on metals. This normalized damage thus determined, we now have an experimental reference necessary for the validation of theoretical models or other approaches of measurement of the experimental damage. It is very interesting to be able to correlate the process of damage to the three stages of damage. By observing the damage curves of Figure-5, we can note the following characteristics.

- At the initiation of the damage, the end of the stage I or the life fraction  $\beta = 30\%$ , the damage increases in a linear and progressive way
- In the slow propagation zone, the stage II which is in the interval of  $\beta = [30\%, 75\%]$  the damage rapidly evolves to 0.8.
- At the moment of the sudden propagation (stage III), the life fraction  $\beta > 75\%$  for  $D = 0.8$ , the damage accelerates very markedly.

Finally, beyond these two intervals, the damage increases in a brutal way.

### Quantification of damage using unified theory

As a method to evaluate the damage taking into account the loading level, the unified theory [10] developed by T. Bui Quoc and al [8] establish a relationship between damage and the loading level. Here, replacing loads by the Young's modulus, normalized damage is written as:

$$D_{th} = \frac{\beta}{\beta + (1 - \beta) \left[ \frac{\gamma - (\gamma/\gamma_u)^m}{\gamma - 1} \right]} \quad (3)$$

$$\text{Where: } \gamma = \frac{E_{Ti}}{E_0} \quad \text{and} \quad \gamma_u = \frac{E_{amb}}{E_0}$$

$E_0$ : Limit of endurance of the material at ambient temperature is equal to the Young's modulus multiplied by a coefficient  $\alpha$  (for  $n=0$ ;  $E_0 = \alpha E_{amb}$ )

$\alpha = \frac{1}{\text{Safety factor}}$  The safety factor is 2, 06 for studied material (ABS) in the industrial zone. Thus, the constant  $m$  is a material parameter, with  $m = 1$  for the amorphous polymers [1].

The variation of unified theory damage and that of the linear Miner rule depending on the fraction of life  $\beta$  are shown in Figure-6. Each curve is associated to a loading level.

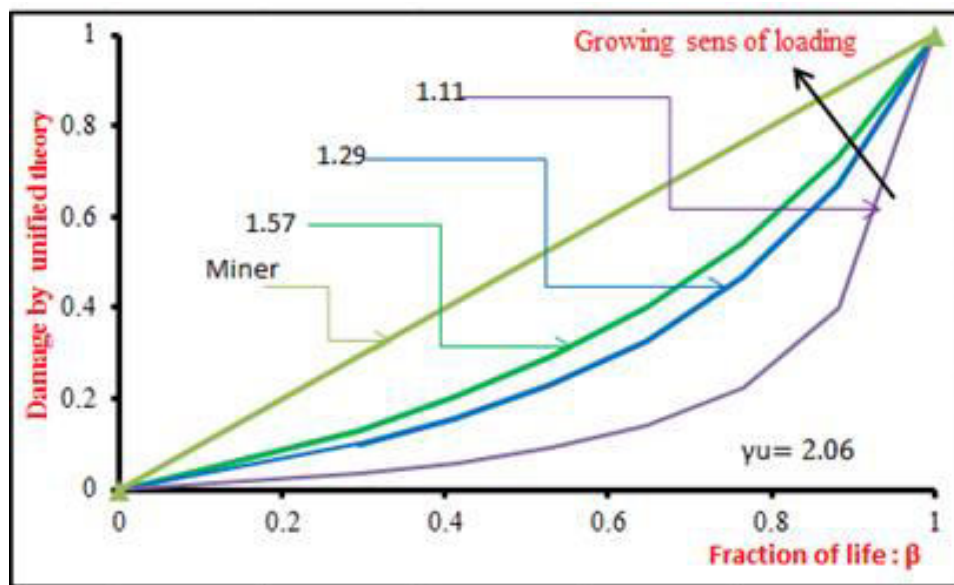


**Figure-6.** Curves Characteristics representing the damage according to the unified theory as a function of fraction of life  $\beta$  for different levels of loading.

From the different curves, which represent the damage according to the unified theory for each loading studied, it can be seen that as the loading increases, the curve of the damage approaches the bisector which corresponds to the damage of Miner. We deduce that Miner's law presents more security since the damage remains underestimated by the computation of damage of the law of the unified theory. Miner's law is more critical with respect to the various damages related to the unified theory.

Hence, the use of the damage defined by the law of Miner in most works dealing with the damage of the structures.

#### Comparison between the static damage and that of Miner and unified

Figure-7 shows the correlation between the damage calculated from equation (2) of static damage and that of the equation (3) of the unified theory, without forgetting the linear rule of Miner.

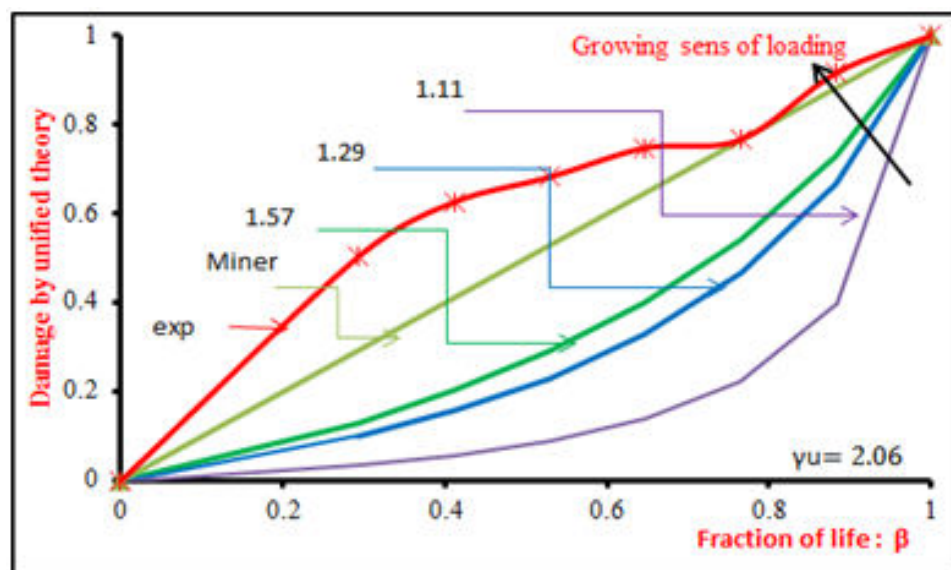


**Figure-7.** Static, unified theory and Miner damage comparison.

In Figure-7 it is found that the experimental damage (static damage) is considered to be the most critical compared to all other damage presented which are considered theoretical.

#### 3.3 Determination of the flow in the thermoforming zone (non-industrial zone $T > T_g$ )

In this zone we define a life fraction  $\beta'$ :





$$\beta' = \frac{T_i - T_g}{T_c - T_g} \quad (4)$$

Where:

T<sub>g</sub>: Glassy temperature

T<sub>c</sub>: Critical temperature

T<sub>i</sub>: Instantaneous temperature

#### Loss of Young's modulus

The variation of the Young's Modulus as a function of the fraction of life β' is described in Figure-8.

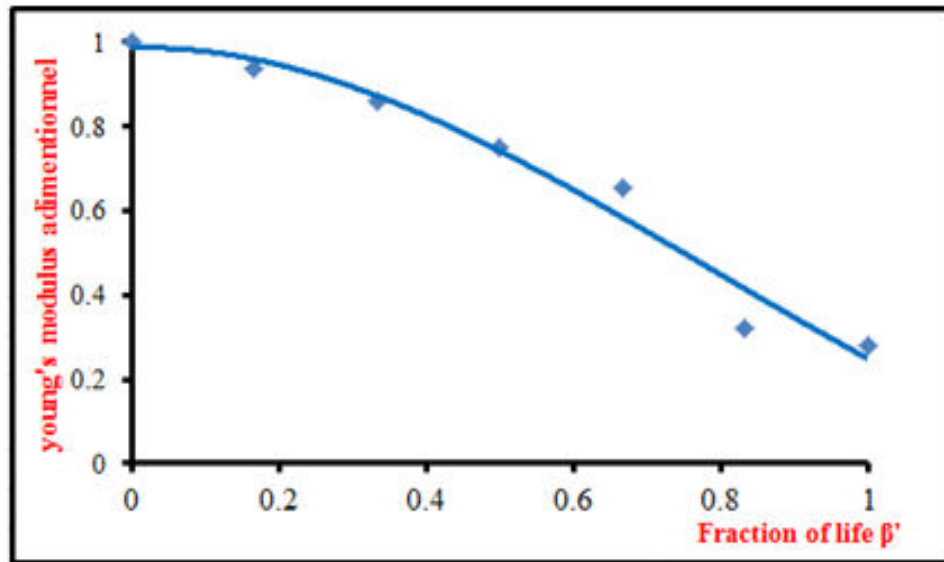


Figure-8. Evolution of the Young's Modulus according to the fraction of life.

We note that the ratio  $E_{T_i} / E_{amb}$  decreases when the temperature of the test piece increases. This normalization allowed us to measure the stress before the rupture which is equal to  $E_a / E_{amb} = 0.23$ .

#### Quantification of static flow

The static flow based on young's modulus, has been developed to predict the flow evolution of the polymer in high temperature ( $T > T_g$ ). The static flow model is presented in the equation (5)

$$F = \frac{1 - \frac{E' T_i}{E' g}}{1 - \frac{E' a}{E' g}} \quad (5)$$

Where:

E'<sub>g</sub>: Value of the Young's modulus at glassy temperature.

E'<sub>T<sub>i</sub></sub>: The value of the Young's modulus for different temperatures in the non-industrial zone

E'<sub>a</sub>: value of the Young's modulus just before the critical temperature.

Figure-9. Illustrate the variation of the flow as a function of the life fraction β' in the thermoforming zone.

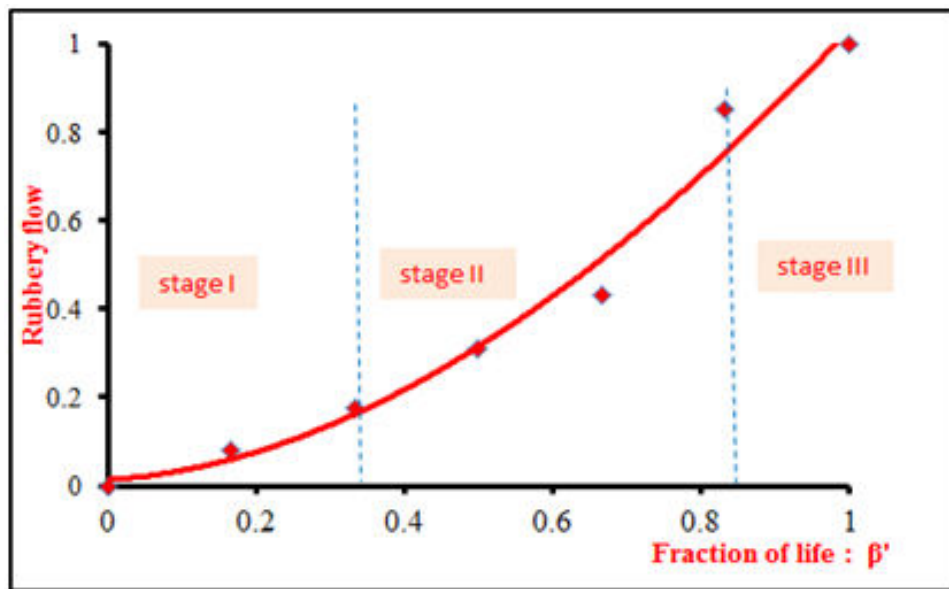


**Figure-9.** Evolution of the rubbery flow as a function of the life fraction  $\beta'$  in the thermoforming zone

Curve 9 illustrates the variation of the flow as a function of the fraction of life  $\beta'$ . We note that the flow increases gradually with the increase in temperature; this is explained by a loss of Mechanical properties caused by an increase in temperature. In fact, the evolution of flow is divided into three stages.

In the first stage ( $0\% < \beta' < 34\%$ ), the flow begins at zero and develops slowly, ie the initiation of the malleability of the ABS material. The second stage ( $34\% < \beta' < 88\%$ ) is characterized by an increase in the flow.

Correspond to the rubbery phase (deformation of the atomic bonds),  $\beta' > 88\%$  begins the third stage, the flow accelerate to have a value of 1 which corresponds to the working area in thermoforming.

#### Quantification of flow using unified theory

By analogy with the unified theory developed by T. Bui Quoc [8] for damage, the equation proposed for the flow of ABS material is:

$$F_{th} = \frac{\beta'}{\beta' + (1 - \beta') \left[ \frac{\gamma' - (\gamma' / \gamma'_u)^m}{\gamma' - 1} \right]} \quad (6)$$

Where:

$\beta'$  = Life fraction

$\gamma' = \frac{E'a}{E'o}$ ;  $E'o$  = limit of endurance of the material in the thermoforming zone

$\gamma'_u = \frac{E'g}{E'o}$ ;  $E'g$  = young's modulus at  $T_g = 110^\circ \text{C}$

Figure-10 shows flow curves by the unified theory in the thermoforming zone.



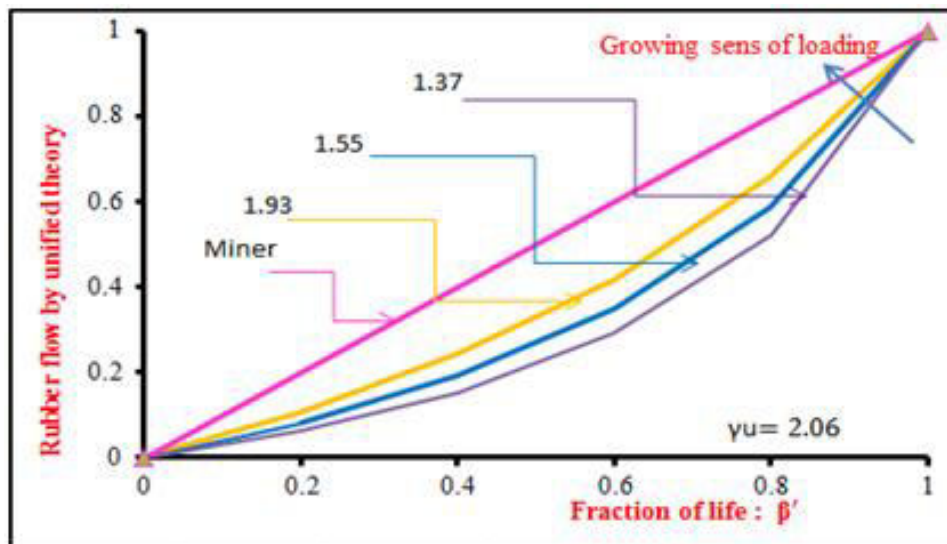


**Figure-10.** Curves Characteristics representing the rubbery flow according to the unified theory as a function of the fraction of life  $\beta'$ .

It is noted that the flow curves approaches gradually the bisector (the linear Miner Law) versus  $\beta'$  for high levels of loading. It is also observed that the curves corresponding to the flow after the vitreous temperature

are almost superimposed and confused with a very small deviation.

#### Comparison between the static flow and that of Miner and unified theory

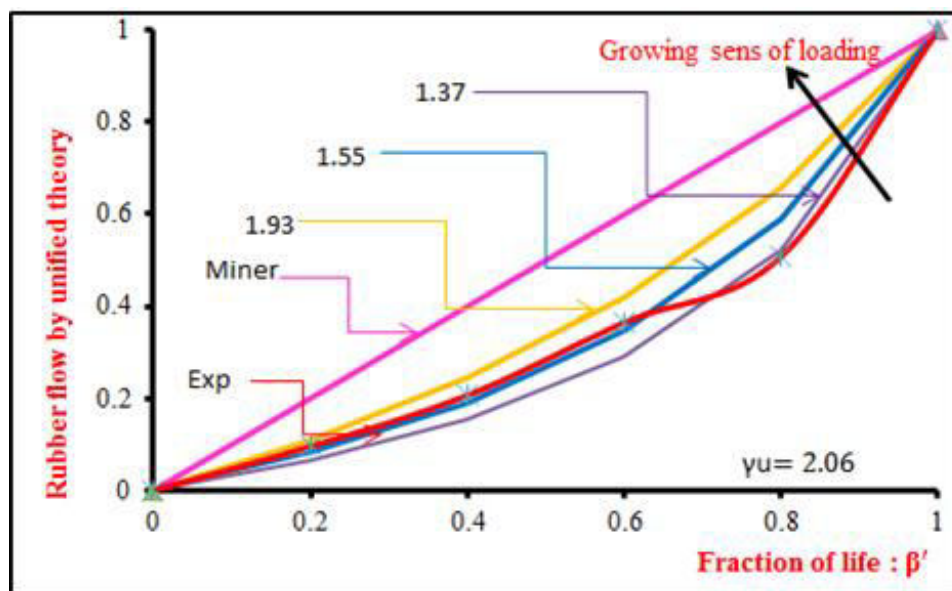


**Figure-11.** Static, unified theory and Miner damage comparison.

Figure-11 shows that the evolution of the static and theoretical flow at a loading level  $\gamma = 1.93$  is similar for low life fractions ( $0\% < \beta < 20\%$ ). With the increase of the life fraction  $\beta$ , the curve of the static flow coincides with that of the unified theory corresponds to the loading level  $\gamma = 1.55$  up to a lifetime  $\beta$  equal to 60%. Then, it exceeds it and becomes coincides with the curve of the unified theory for a loading level  $\gamma = 1.37$  at the end of the stage II.

In Stage III, the static and theoretical flow curves ( $\gamma = 1.37$ ) are similar. It remains to be noted that the graphs of the two types of flows remain below the Miner-given torque.

Therefore, it can be concluded that the static flow is less dangerous compared to all the courses presented in the thermoforming zone. We deduce that the flow presented by the law of MINER presents more security with respect to the flow calculate by the unified theory.



#### 4. CONCLUSIONS

The unified theory has been used in two areas: the industrial zone and the thermoforming zone to give a more complete model that can more accurately describe the state of the material.

In the industrial zone, we used the unified theory, which is formulated in a macroscopic approach to damage. We have first redefined the different parameters of the model according to our type of traction load. Thus reformulated, the validity of this one is implemented during a comparative study between the theoretical predictions and the experimental measurements. We have seen that the theoretical predictions are more or less close to the experimental results.

In the thermoforming zone, we adapted the unified theory of damage to the flow. We first redefined the different parameters of the model according to our work area. The theoretical method has also been confirmed by the calculation of the static damage based on the experimental measurements of the Young's modulus which varies with the variation of the temperature. We have also observed that the theoretical predictions are very close to the experimental results.

This comparative study made it possible to reveal that the predictions of our theoretical model of damage and flow are not significant for low loadings. On the other hand, for large loadings, theoretical predictions are closer to those obtained via experimental measurements.

The results showed the feasibility of the applied damage approach. The proposed approach involves intrinsic parameters of the material (its Young's model, its temperature), which allows a rigorous description of the damaging state of the materials.

These preliminary studies are essential steps for the full realization of our medium-term objectives of the implementation and development of tools for the modeling and simulation of thermoplastic forming processes.

#### REFERENCES

- [1] R. RHANIM. 2016. Mechanical behavior Study of damaged structures of polymers. Digital Calculation / Testing Dialogue. Application to photoelasticimetry.
- [2] Mechanical behavior of polymers.
- [3] B. Ni, J. Li et V. Berry. «Plastic zone in front of a mode I crack in acrylonitrile-butadiene-styrene.
- [4] The ABS data sheet.
- [5] Makadir, M. Barakat, M. Elghorba, H. Farid. 2015. Study of Damage to ABS Specimens Submitted To Uniaxial Loading. The International Journal of Engineering and Science (IJES). 4(1): 05-08.
- [6] ASTM D638-03 Standard test method for tensile properties of plastics.
- [7] F. Hicham. 2015. Behavior and damage of membranes thermoplastics in large deformations.
- [8] C. Bathias, J. Bailon. 1980. The fatigue of materials and structures. pp. 328-330.
- [9] N.Mouhib *et al.* 2015. Tensile test of a strand with 2 broken wires artificially damaged.
- [10] M. Chahid, G. M. El, M. Benhamou et Z. Azari. 1996. «Reliability optimization of fatigue damage of a glass-epoxy composite material. »Materials and techniques. 84: 13-17.